Research & Reviews: Journal of Material Sciences e-ISSN: 2321-6212

Study of Hollow ZnO Nanoparticles By Flame Spray Synthesis

Li Hui*

Department of Physics, Xijing University, Xi'an, China

Research Article

Received: 11-Feb-2022, Manuscript No. JOMS-22-54232; **Editor assigned:** 13-Feb-2022, PreQC No. JOMS -22-54232(PQ); **Reviewed:** 25-Feb-2022, QC No. JOMS -22-54232; **Revised:** 27-Feb-2022, Manuscript No. JOMS -22-54232(R); **Published:** 06-Mar-2022, DOI: 10.4172/2321-6212.10.2.005.

***For Correspondence:**
Li Hui, Department of Physics, Xijing University, Xi'an, China
E-mail: lzlihui@126.com

Keywords: Hollow ZnO; Nanoparticles; Optical properties

ABSTRACT

Hollow ZnO nanoparticles prepared by Flame Spray Synthesis (FSP) have been reported in this letter. By the results obtained from X-Ray Diffraction (XRD) pattern and High-Resolution Transmission Electron Microscopy (HR-TEM) picture, it is concluded that the hollow ZnO nanoparticles were successfully synthesized at high temperature.
The size of hollow nanoparticles distributed between 20 and 30 nm, and the formation mechanism of this hollow structure was discussed in the synthesis process. The strong Ultra-Visible (UV) emission was shown in Photoluminescence (PL) spectra, while the mechanism had been explained in detail.

INTRODUCTION

Due to its broad band-gap energy, lost effective, physicochemical stability, easiness of availability and high oxidative capacity, ZnO based nanocomposites have received much attention in the last decades. Owing to their low density, large outer-and-inner surface as well as cavity-confined nanoscale reactions and transport process, ZnO nanostructure materials have wide potential application in the areas of photocatalyst, anti-bacteria, biomedical diagnosis, air ventilation and water purification[1-8].

Environmental pollution has become a major challenge for the development of modern human society; therefore the waste water treatment utilizing environmental friendly photocatalyst has been extensively studied. In order to explore the potential of ZnO nanostructure materials, crystalline morphology, orientation and surface architecture of nanostructure can be well controlled during the preparation process. The simplest hollow nanostructures are ZnO nanotubes shells and nanoparticles[4,7]. Until now, it was proposed by many useful methods for synthesis ZnO nanoparticles. Since Wong et al. showed the quantum confinement of photoluminescence in ZnO nanoparticles by Electrophoretic Deposition (EPD)[9], Usui et al. investigated the defect emission of ZnO nanoparticles using different surfactant by laser ablation and Demangeot et al. reported the UV emission potential of ZnO nanoparticles by using organometallic method[10,11]. By these synthesis methods, the size of nanoparticles distributed within a range between several nanometers to several hundred nanometres. At the same time, our group developed the technique of flame spray synthesis and made some progress on the research of optical properties of undoped, Mg and In doped ZnO nanoparticles[12], which was based on the work of T. Tani who grew metal-oxide nanoparticles with high melting point by flame spray synthesis[13,14]. Otherwise, the hollow nanoparticles prepared by flame spray synthesis have rarely been reported. In this paper, we prepared hollow ZnO nanoparticles by the improved flame spray apparatus and discussed the formation mechanism of hollow ZnO nanoparticles at high temperature.

On the other side, although ZnO material has large binding exciton energy of 60 meV, the luminescent mechanism of ZnO nanoparticles is still a controversial issue for optical device. The luminescence was strongly depended on crystalline size [15-16], surface oxygen-related defects and some impurities in the nanoparticles [17-19]. These different factors will result in the intensity of UV emission weak and be suppressed at room temperature. Therefore, the optical properties of hollow ZnO nanoparticles are also currently of great scientific and technical significance. In this paper we will also discuss photoluminescence phenomenon of the sample.

MATERIALS AND METHODS

The schematic of improved apparatus was shown in Figure 1. In the synthesis process, it was used hydrogen gas as combustible gas instead of common gas such as methane or acetylene, which could avoid the formation of carbide impurities at the surface of nanoparticles. The selected precursors mixture was zinc acetate [$Zn(CH_3COOH)_2 \cdot 2H_2O$, $ZnAc_2 \cdot 2H_2O$], which was dissolved in ionized water stirring for 3 h at room temperature. The solution of 0.05mol/L was set into an ultrasonic sprayer, which substituted common syringe in flame spray pyrolysis of former paper[12]. The preparation process was as follow: A vapour stream carrying $ZnAc_2 \cdot 2H_2O$ was continuously introduced into a nozzle, combusting in the oxyhydrogen flame (H_2:O_2=2:1, the increasing ratio of hydrogen to oxygen could get higher temperature in the inner flame).

Figure 1. The schematic diagram of flame sprays synthesis apparatus.

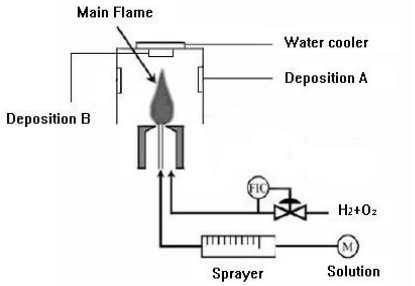

A vertical quartz tube was placed onto oxyhydrogen flame to collect the combusted sample. The precursors burning in outer flame deposited in Deposition A, which was composed of solid ZnO nanoparticles, and the morphology picture was same as the sample previously reported [12]. In the top of tube, the samples in this paper deposited in deposition B where a water cooler was equipped with.

The ZnO material structures were obtained by X-Ray diffraction (Rigaku D/Max-IIIC CuKα ray), and the morphology of samples were investigated by high-resolution field emission transmission electron microscopy (TEM, Tecani F30 from FEI Company). The Photoluminescence (PL) spectra were performed using a UV He-Cd laser excitation source with 325 nm wavelength at room temperature (300 K).

RESULTS AND DISCUSSION

Figure 2 presented the XRD patterns of hollow ZnO nanoparticles by flame spray synthesis deposited in Deposition B. The sharp diffraction peaks matched well with the pattern of standard hexagonal structure of ZnO nanoparticles. The most strong peaks locating at 31.58°, 34.62°and 36.02°are seen clearly in the XRD pattern of ZnO nanoparticles, which were corresponding to the (100), (002) and (101) directions of ZnO, respectively. Except for three most obvious peaks, the other peaks contained (102), (110), (103), (200), (112), (201), (004) and (202) of ZnO could be indexed from the hexagonal ZnO XRD pattern of JCPDS.

According to the Bragger Law,

$$2d\sin\theta = n\lambda$$

the lattice constants a and c of wurtzite structure ZnO were calculated by

$$\frac{1}{d^2_{hkl}} = \frac{4}{3}\left(\frac{h^2 + hk + k^2}{a^2}\right) + \frac{l^2}{c^2}$$

With the first order approximation n=1 for the (100) orientation, the lattice constant a was derived as

$$a = \frac{\lambda}{\sqrt{3}\sin\theta}$$

and for the (002) orientation, the lattice constant c was calculated as ,

$$c = \frac{\lambda}{\sin\theta}$$

The calculated lattice constant a was 0.3268 nm and c was 0.5231 nm. The mean grain size (S) of samples could be calculated by Scherrer's formula,

$$d = \frac{0.9\lambda}{B\cos\theta_B}$$

where λ, θ_B and B are the X-ray wavelength, Bragg diffraction angle, and line width at half maximum, respectively. The grain size(S) was evaluated around 25 nm in different directions of (100) and (101).

Figure 2. The XRD pattern of hollow ZnO nanoparticles.

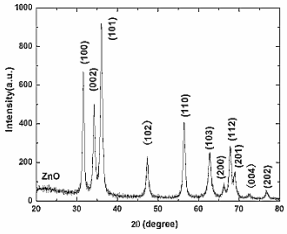

Figure 3 depicted the TEM pictures of samples deposited in deposition B, where it was equipped a water cooler. As shown in Figure 3(A), the samples were all nearly composed of hollow nanoparticles with the size of 20 nm, which were different from the solid nanoparticles by flame spray synthesis in the former report [12]. By the Microbeam Electron Diffraction (MBED) pattern in Figure 3(B), it could be seen in the insert figure that the surface of hollow particle was in the direction of (100) and (101), which was consistent with the result of ZnO XRD pattern in Figure 1.

Figure 3. TEM images of hollow ZnO nanoparticles and corresponding MBED pattern in the insert figure.

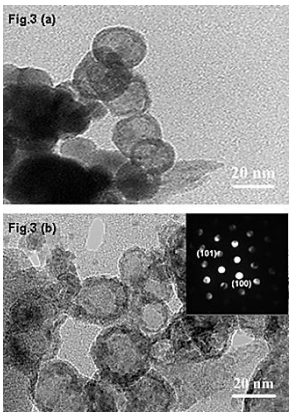

Compared with the nanoparticles formed in other paper in deposition A, it was just briefly discussed the formation mechanism of ZnO hollow nanoparticles. As shown in Figure 4, the $ZnAc_2 \cdot 2H_2O$ was firstly dissolved in deionized water, and small Zn^{2+} was formed in water stirring for some while. Along with the vapour steam by ultrasonic sprayer, small Zn^{2+} droplet was transported into the oxyhydrogen flame. Because the combusting temperature was lower in out flame than that of inner flame temperature, the tiny particles formed ZnO nanoparticles after undergoing reaction with oxygen. Then, the ZnO nanoparticles aggregated firmly to form clusters and deposit in deposition A, where the morphology of nanoparticles could be found in previous paper [12]. Some small Zn^{2+}

combusted in inner flame, where the highest temperature of oxyhydrogen flame could reach at 3000K. Higher temperature was in favour of the reacted ZnO expending to form hollow sphere structure, which deposited in Deposition B of Figure 1. The morphology was reflected in the TEM picture of Figure 3(A). There was some possibility that there was some Zn^{2+} not reacting with oxygen in short time, which was surrounded by ZnO tiny particles and deposited in the top of tube, whose morphology was corresponding to small solid particles in TEM picture of Figure 3.

Figure 4. The formation process of hollow ZnO nanoparticles by flame spray synthesis.

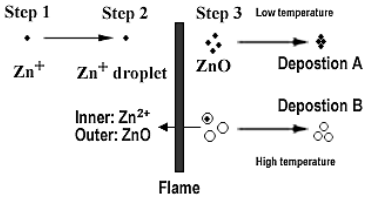

We also discussed the PL spectra of hollow nanoparticles measured at room temperature in Figure 5. Firstly, it was explained the weak visible emission. It was found that the weak visible emission was located at around the wavelength of 550 nm. In the previous paper, it was attributed to Oxygen Vacancy (VO) or Znic Interstitial (Zni) when the sample was short of oxygen content in the preparation process [12]. As the ratio of hydrogen to oxygen increased (H_2:O_2=1:1 and H_2:O_2=2:1) the combusted temperature increased in the inner flame especially. However, when the morphology of particle changed from solid into hollow in the same size range, the location of visible emission didn't change to some extent. In the former reports, there were also reported a broad visible emission located 550 nm, which was originated from the VO located near the surface region[18,20]. In our experiment, the location of visible emission was same as the results of them. This result was different from other defects discussion on visible emission of ZnO powder and ZnO nanoparticles in SiO_2 by ion implantation combined with thermal oxidation [21-23], where the visible emission usually located around 520 nm. Therefore, it was attributed the 550 nm emission to surface absorption defects in the size of 20 nm range after precursors oxidation at room temperature.

The Figure 5 also depicted the Near-Band-Edge (NBE) emission in UV area centred at around the wavelength of 360 nm (The peak was corresponded with 3.35 eV). The energy of NBE emission was lower than the band gap (3.38 eV), which was same as that of the solid ZnO nanoparticles. It was considered that the NBE emission had some relation with exciton emission as same as other papers about ZnO nanomaterials. Compared with solid nanoparticles, the intensity of hollow nanoparticles increased to some extent, while the intensity of visible emission nearly changed a little. On one side, the exciton effect in nano-hollow structures was stronger than that of bulk and film materials at room temperature, and the former structure was in favour of fulfilling exciton emission near the band edge. At low temperature, this prominent effect happened much evident. On the other side, the high temperature of oxyhydrogen flame could decrease the defects adsorbed at the surface of nanoparticles, which usually suppressed the NBE exciton emission. Therefore, in our paper the NBE emission of hollow ZnO nanoparticles was stronger in evidence than that of other reports [18-20].

Figure 5. The PL spectra of hollow ZnO nanoparticles at room temperature.

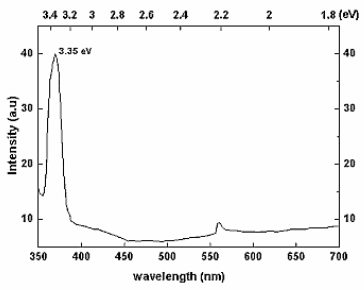

CONCLUSION

The hollow ZnO nanoparticles were successfully prepared by improved flame spray synthesis at high temperature. High-resolution field emission TEM analysis revealed that the size of hollow particle ranged between 20-30 nm. It was discussed the reason of increasing NBE emission by exciton effects, and weak visible emission by the defects in the surface of hollow nanoparticles which was produced in the process of preparation.

REFERENCES

1. Chng LL, et al. Nanostructured catalysts for organic transformations. Acc Chem Res. 2013; 46:1825.
2. Duan X, et al. Orientable pore-size-distribution of ZnO nanostructures and their superior photocatalytic activity. Cryst Eng Comm. 2010; 12:2821.
3. Sun T, et al. Controllable fabrication and photocatalytic activity of ZnO nanobelt arrays. J Phys Chem C. 2008; 112:715.
4. Wang HQ, et al. Controllable preferential-etching synthesis and photocatalytic activity of porous ZnO nanotubes. J Phys Chem C. 2008; 112:11738.
5. Zheng Y, et al. Luminescence and photocatalytic activity of ZnO nanocrystals: Correlation between structure and property. Inorg Chem. 2007; 46:6675.
6. Wu D, et al. Hierarchical ZnO aggregates assembled by orderly aligned nanorods for dye-sensitized solar cells. Cryst Eng Comm. 2013; 15:1210.
7. Lu X, et al. Efficient photocatalytic hydrogen evolution over hydrogenated ZnO nanorod arrays. Chem Commun. 2012; 48:7717.
8. Sun K, et al. 3D branched nanowire heterojunction photoelectrodes for high efficiency solar water splitting and H2 generation. Nanoscale. 2012; 4:1515.
9. Wong EM, et al. ZnO quantum particle thin films fabricated by electrophoretic deposition. Appl Phys Lett. 1999; 74:2939.
10. Usui H, et al. Photoluminescence of ZnO nanoparticles prepared by laser ablation in different surfactant solutions. J Phys Chem B. 2005; 109:120.
11. Demangeot F, et al. Experimental study of LO phonons and excitons in ZnO nanoparticles produced by room-temperature organometallic synthesis. Appl Phys Lett. 2006; 88:071921.
12. Li H, et al. Effects of In and Mg doping on properties of ZnO nanoparticles by flame spray synthesis. J Nanopart Res. 2009; 11:917.
13. Tani T, et al. Homogeneous ZnO nanoparticles by flame spray pyrolysis. J Nanopart Res. 2002; 4:337.
14. Tani T, et al. Evolution of the morphology of zinc oxide/silica particles made by spray combustion. J Am Ceram Soc. 2004; 87:365.
15. Fu ZD, et al. Study on the quantum confinement effect on ultraviolet photoluminescence of crystalline ZnO nanoparticles with nearly uniform size. Appl Phys Lett. 2007; 90:263113.
16. Yoshikawa M, et al. Characterization of ZnO nanoparticles by resonant Raman scattering and cathodoluminescence spectroscopies. Appl Phys Lett. 2008; 92:113115.
17. Lee CY, et al. Electroluminescence from monolayer ZnO nanoparticles using dry coating technique. Appl Phys Lett. 2008; 92:261107.
18. Ghosh M, et al. Ionic environment control of visible photoluminescence from ZnO nanoparticles. Appl Phys Lett. 2008; 93:123113.
19. Peng WQ, et al. Synthesis and temperature-dependent near-band-edge emission of chain-like Mg-doped ZnO nanoparticles. Appl Phys Lett. 2006; 88:101902.
20. Shalish I, et al. Size-dependent surface luminescence in ZnO nanowires. Phys Rev B. 2004; 69:245401.
21. Vanheusden K, et al. Mechanisms behind green photoluminescence in ZnO phosphor powders. J Appl Phys. 1996; 79:7983.
22. Amekura H, et al. Fabrication of ZnO nanoparticles in SiO_2 by ion implantation combined with thermal oxidation. Appl Phys Lett. 2005; 87:013109.
23. Amekura H, et al. Zn and ZnO nanoparticles fabricated by ion implantation combined with thermal oxidation and the defect-free luminescence. Appl Phys Lett. 2006; 88:153119.